TOXICOLOGICAL SCIENCES **115(1)**, 109–117 (2010)
doi:10.1093/toxsci/kfq023
Advance Access publication January 27, 2010

Long-term AZT Exposure Alters the Metabolic Capacity of Cultured Human Lymphoblastoid Cells

Ofelia A. Olivero,*[,1] Irma L. Vazquez,* Catherine C. Cooch,* Jessica Ming,* Emily Keller,* Mia Yu,* Jennifer P. Borojerdi,* Hannan M. Braun,* Edward McKee,† and Miriam C. Poirier*

*Carcinogen-DNA Interactions Section, National Cancer Institute, National Institutes of Health, Bethesda, Maryland 20892-4255; and †South Bend Center for Medical Education, Indiana School of Medicine, Notre Dame, Indiana 46556

[1] To whom correspondence should be addressed at Laboratory of Cancer Biology and Genetics, Carcinogen-DNA Interactions Section, National Cancer Institute, National Institutes of Health, 37 Convent Dr. MSC 4255, Bldg 37 Rm 4032, Bethesda, MD 20892-4255. Fax: (301) 402-0153. E-mail: oliveroo@exchange.nih.gov.

Received October 23, 2009; accepted January 21, 2010

The antiretroviral efficacy of 3′-azido-3′-deoxythymidine (AZT) is dependent upon intracellular mono-, di-, and triphosphorylation and incorporation into DNA in place of thymidine. Thymidine kinase 1 (TK-1) catalyzes the first step of this pathway. MOLT-3, human lymphoblastoid cells, were exposed to AZT continuously for 14 passages (P_1–P_{14}) and cultured for an additional 14 passages (P_{15}–P_{28}) without AZT. Progressive and irreversible depletion of the enzymatically active form of the TK-1 24-kDa monomer with loss of active protein was demonstrated during P_1–P_5 of AZT exposure. From P_{15} to P_{28}, both the 24- and the 48-kDa forms of TK-1 were undetectable and a tetrameric 96-kDa form was present. AZT-DNA incorporation was observed with values of 150, 133, and 108 molecules of AZT/10^6 nucleotides at the 10μM plasma-equivalent AZT dose at P_1, P_5, and P_{14}, respectively. An exposure-related increase in the frequency of micronuclei (MN) was observed in cells exposed to either 10 or 800μM AZT during P_1–P_{14}. Analysis of the cell cycle profile revealed an accumulation of S-phase cells and a decrease in G_1-phase cells during exposure to 800μM AZT for 14 passages. When MOLT-3 cells were grown in AZT-free media (P_{15}–P_{29}), there was a reduction in AZT-DNA incorporation and MN formation; however, TK-1 depletion and the persistence of S-phase delay were unchanged. These data suggest that in addition to known mutagenic mechanisms, cells may become resistant to AZT partially through inactivation of TK-1 and through modulation of cell cycle components.

Key Words: **nucleoside analog; antiretrovirals; thymidine kinase.**

The genotoxicity of the DNA chain–terminating nucleoside reverse transcriptase inhibitors (NRTIs) has been amply demonstrated (International Agency for Research on Cancer, 2000), but specific underlying mechanisms other than DNA incorporation and mutagenesis are unclear. Since clinical NRTI therapy is administered long term and because human bone marrow is a target for NRTI toxicity (Richman *et al*., 1987; Yarchoan *et al*., 1989), human lymphoblastoid (MOLT-3) cells were used here to study the genotoxic mechanisms of long-term NRTI exposure. It is well established that 3′-azido-3′-deoxythymidine (AZT) acts as an HIV-1 reverse transcriptase inhibitor (Mitsuya *et al*., 1985) by DNA incorporation that is required for chain termination and by blocking the nucleotide-binding site of the HIV-1 reverse transcriptase (Furman *et al*., 1986).

Thymidine kinase 1 (TK-1) catalyzes the monophosphorylation of AZT in the pathway of activation to DNA incorporation and is considered to be the rate-limiting step in NRTI metabolism. In cultured human cells, AZT resistance has been reported to be correlated with decreases in TK-1 activity (Avramis *et al*., 1993; Han *et al*., 2004) and hypermethylation of the *TK1* gene (Nyce *et al*., 1993; Wu *et al*., 1995). TK-1 exists intracellularly as an active monomeric form (24 kDa), an inactive dimeric form (48 kDa), and an inactive cytosolic tetramer (96 kDa) (Sherley and Kelly, 1988).

The triphosphorylated AZT becomes incorporated into virus and host DNA in place of thymidine, inducing chain termination that results in DNA fragmentation and the formation of micronuclei (MN) (Olivero, 2007). Induction of MN occurring as a result of exposure to AZT has been reported in many different studies using various cell cultures and animal species. For example, increased levels of MN were reported in CD4 lymphocytes (Stern *et al*., 1994) and human lymphocytes and Chinese hamster ovary cells (Gonzalez and Larripa, 1994), HeLa cells (Aruna and Jagetia, 2001), and human H9 cells (Agarwal and Olivero, 1997) all as a result of exposure to AZT. In addition, an increase in frequency of erythrocyte MN was observed in mouse pups exposed to AZT plus the NRTI didanosine (ddI) during gestation and after birth (Bishop *et al*., 2004; Dertinger *et al*., 1996; Witt *et al*., 2004) and in TK $^{+}/^{+}$ and TK $^{+}/^{-}$ mice (Dobrovolsky *et al*., 2005). The formation of AZT-DNA incorporation and AZT-induced MN suggests that chronic AZT exposure may induce mutations and functional

alterations in DNA replication. Increase in the frequency of complete *Tk* gene deletions following exposures to AZT and ddI have been reported (Meng *et al*., 2002) *in vitro* and *in vivo* (Von Tungeln *et al*., 2004). Furthermore, mutational analysis suggests that AZT induces a unique pattern of mutations in the *Tk* gene of mice and that the major mechanisms of AZT-induced mutagenesis involve deletion and recombination (Mittelstaedt *et al*., 2004).

Here, we pursued mechanistic studies exploring consequences of prolonged AZT exposures using high concentrations of AZT that have been shown to induce genotoxicity and minimum cell death and compared those to therapeutic doses. Additionally, we have explored the persistence of AZT-induced effects once the exposure was terminated. To this end, we cultured MOLT-3 cells continuously in the presence of AZT for 14 passages (P_{14}), followed by an additional 15 passages in the absence of the drug. We explored cell cycle parameters by flow cytometry and DNA damage by a radioimmunoassay (RIA) able to detect AZT incorporated into DNA and by documenting MN formation. Additionally, we investigated the role of chronic AZT exposure as a modulator of TK-1 oligomerization and functional capacity.

MATERIALS AND METHODS

Cell culture and treatment. The human lymphoblastoid cell line MOLT-3 (ATCC, Manassas, VA) was cultured using Rossman-Park-Memorial-Institute (RPMI) 1640 medium supplemented with 10% fetal bovine serum (ATCC). AZT (Sigma-Aldrich Co., St Louis, MO) exposures were performed in 75-cm^2 plastic culture flasks. AZT was dissolved in PBS (pH 7.2) (Biosource, Rockville, MD), and the final concentration was calculated from absorbance at 266 nm with a molar extinction coefficient of 11,500. Triplicate experiments were performed to assess the incorporation of 0, 5, 10, 50, 100, 200, and 800μM AZT into MOLT-3 cell DNA, for up to 14 passages. In a separate study, five different batches of MOLT-3 cells were exposed continuously to 800μM AZT for up to P_{14}, and for three of those five experiments, AZT was removed at P_{14} and cells were grown for an additional 15 passages (to P_{29}) in the absence of drug. Finally, in a repeat experiment, MOLT-3 cells were exposed to 10μM AZT, a human plasma level concentration, for 14 passages.

Throughout this study, unexposed cells, cultured simultaneously and in parallel with every experimental passage, were used as controls for the end points examined. To simplify the written explanation, we have designated all unexposed passages as "P_U"; however, it is important to recognize that for each experiment an appropriate unexposed control of the same passage was used for comparison.

Cytotoxicity analysis and time to subculture. MOLT-3 cells, from five independent trials, were collected 24 h after exposure to either 0 or 800μM AZT. For each experiment, cells were counted twice in a Coulter Counter (Coulter Electronics Limited, UK), and cell counts from drug-exposed flasks were compared with those from the unexposed flasks. Survival in exposed cells was expressed as percentage of survival in unexposed cells. In addition to counting, survival was established by trypan blue exclusion, with numbers of viable cells compared in exposed and unexposed cells. A separate observation was made in 15 independent trials to establish time to subculture. The ability of the cells to proliferate was also evaluated based on color changes in the culture medium indicated by phenol red. Typically, a yellowish color is observed when a critical amount of cells is present, point at which the cells were subcultured.

Preparation of DNA and measurement of AZT incorporated into DNA by RIA. DNA from unexposed cells and AZT-exposed cells at P_1, P_5, and P_{14} was obtained by nonorganic isolation (Chemicon International, Temecula, CA). The incorporation of AZT into MOLT-3-DNA was determined in cells exposed to 0, 5, 10, 50, 100, 200, and 800μM AZT by an AZT-RIA (Olivero *et al*., 1994). Briefly, a rabbit polyclonal anti-AZT antibody (Sigma-Aldrich Co.), which also recognizes AZT in DNA (Olivero *et al*., 1994), was reconstituted, diluted 1:7500, and incubated with MOLT-3-DNA for 90 min at 37°C. An aliquot (100 μl) containing ~20,000 cpm of [^{3}H]AZT tracer (16 Ci/mmol; Moravek Biochemicals Inc., Mountain View, CA) was added to each tube together with 100 μl of the secondary antibody, goat anti-rabbit immunoglobulin G (IgG; Sigma-Aldrich Co.), and reconstituted in 12 ml of 2-amino-2-hydroxymethyl-propane-1,3-diol (Tris) buffer (pH 8.00). The mixture was incubated for 25 min at 4°C, centrifuged at 1942 × g for 15 min at 4°C, and the resulting supernatant was decanted. The pellets were dissolved in 200 μl 0.1M NaOH, transferred to scintillation vials containing 6 ml Ecolite (MP, Irvine, CA), and counted in a liquid scintillation counter. The amount of standard AZT, added to 3 μg of unexposed carrier MOLT-3-DNA, required to inhibit antibody binding by 50% was 2.86 ± 0.9 (average ± SD, $n = 12$) pmol AZT/tube. The lower limit of detection was 4.2 molecules of AZT/10^6 nucleotides.

MN assay. In separate experiments, MOLT-3 cells were exposed to 0, 10, and 800μM AZT and collected at P_1, P_4, P_5, and P_{14}. MOLT-3 cells, exposed on three separate occasions to 0 and 800μM AZT, were collected at P_1, P_4, P_5, P_{14}, and P_{27}. Cells from all the treatments and unexposed cells were centrifuged and pellets were fixed with 70% alcohol to obtain suspensions of 8×10^4 cells/ml media. Ten slides/passage/experiment were obtained by centrifugation of 50 μl of the cell suspension/slide (~4000 cells) using a cytocentrifuge (Shandon Cytospin 2; Thermo Fisher Scientific Inc., Waltham, MA). Cells were stained with a 5% solution of Giemsa stain in PBS (pH 7.4) for 5 min. MN were scored in 1000 MOLT-3 cells from 10 slides/passage.

Flow cytometric analysis of cell cycle parameters. MOLT-3 cells were exposed on three separate occasions to 800μM AZT during P_1–P_{14} and then grown in AZT-free media for additional 10 passages. Cells were collected at every passage, pelleted, and washed with RPMI 1640 without serum before they were fixed in 1 ml 70% ice-cold ethanol, gently dropped while vortexing. Following an overnight fixation at 4°C, cells were pelleted by centrifugation and incubated with Ribonuclease A (Sigma-Aldrich Co.) at room temperature for 20 min. Propidium iodide (20–50 μg/ml) (Molecular Probes, Eugene, OR) was added to each cell suspension, and cells were kept in the dark at 4°C overnight. Cells were passed through a fluorescence-activated cell sorter (FACSCalibur; BD Biosciences, San Jose, CA) using the doublet discrimination module, and data were acquired using CellQuest (BD Biosciences) software. The cell cycle was modeled using ModFit software (Venty Software, Topsham, ME). Percentages of cells in G_0–G_1, S, and G_2–M phases were calculated directly by the software.

Western blot for TK-1 protein analysis. Aliquots of unexposed and AZT-exposed MOLT-3 cells from each passage were lysed in radio-immune precipitation assay buffer (50mM Tris-HCl [pH 7.6], 150mM NaCl, 0.25% SDS, 1% Triton X-100, 1mM EDTA, and 0.5% Nonidet P-40 [NP-40]; Fluka Chemicals, Milwaukee, WI) with the addition of protease inhibitor tablets (Complete; Roche Diagnostics, Indianapolis, IN) for 30 min on ice, followed by sonication with an ultrasonic processor at a 20% amplitude with a 3-mm microtip (Sonics VC 750; Sonics and Materials Inc., Newtown, CT) for three pulses of 10 s each. Proteins were quantified by Bradford reaction (Bio-Rad, Hercules, CA). Samples were resolved on a 10% Bis-Tris vertical polyacrylamide gel (NuPage; Invitrogen) and then transferred to a polyvinylidene fluoride membrane (Immobilon-P; Millipore, Billerica, MA). Membranes were allowed to dry overnight and then were blocked with phosphate buffer saline 0.1% tween containing 5% nonfat dry milk. A TK-1 monoclonal antibody (QED Biosciences, San Diego, CA) was used to incubate the membrane overnight at 4°C. After incubation with an anti-mouse IgG-horseradish peroxidase (HRP)–conjugated secondary antibody (Novus Biologicals, Littleton, CA), the membrane was processed for chemiluminescence with an Enhanced Chemiluminescence

Western Blotting Detection Kit (Amersham Biosciences, Buckinghamshire, UK). Controls for loading were carried out after stripping the membrane (Restore; Invitrogen) using a mouse anti-actin antibody (Chemicon International) followed by an anti-mouse IgG-HRP–conjugated secondary antibody (Novus Biologicals). Signal was revealed using electrochemiluminescence Western Blotting Detection Reagents as previously described (Olivero *et al*., 2008). Images were captured using a Lumi-imager (Roche Diagnostics).

Radiochemical enzyme–specific activity assay for TK-1. Pellets from AZT-exposed cell suspensions (3×10^7 cells) collected at different passages in three separate experiments were resuspended in 1 ml of ice-cold extraction buffer (50mM Tris-HCl [pH 7.6], 2mM dithiothreitol [DTT], 1 protease inhibitor cocktail tablet [Roche Diagnostics], 20% glycerol, and 0.5% NP-40). Cell suspensions were frozen and thawed three times to improve the lysis process, and sonicated cell lysates were centrifuged for 10 min at 18,000 × g at 4°C. The supernatant was kept on ice and analyzed for protein concentration as described above using the Bradford reaction. Diethylaminoethyl cellulose filter discs (Whatman, Maidston, UK) were immersed in 10μM AZT-monophosphate (MP) for 10 min and allowed to dry completely. The reaction mixture (50mM Tris-HCl [pH 7.6], 2mM DTT, 5mM $MgCl_2$, 5mM ATP, 10mM NaF, and 20μM [H^3]-AZT; 12 Ci/mmol; Moravek Radiochemicals, Brea, CA) was used to incubate the protein extract at 37°C for 20 min. After that time, 20 μl of the suspension was spotted on the pretreated DEAE discs. The discs were allowed to air dry and washed three times with ammonium formate, transferred to liquid scintillation vials, and eluted with 0.1M HCl + 0.2M NaCl solution for 30 min to release the [^{3}H]-AZT-MP. The eluate was diluted in liquid scintillation solution, and radioactivity was counted. TK-1 activity (counts per minute) was measured as directly proportional to the radioactivity obtained (Arner *et al*., 1992).

Phosphorylation of [^{3}H]-thymidine during cell growth. Control cells and cells treated with 800μM AZT for 1, 45, and 59 passages were incubated for 30 min with [^{3}H]-thymidine. Cells were harvested and lysed in 5% trichloroacetic acid. After 10 min on ice, the extracts were centrifuged at a 3-min centrifugation at 2000 × g at 4°C. A measured volume of the resultant supernatant was neutralized by addition of AG-11A8 resin (0.5 g/ml extract), filtered, and the labeled deoxynucleoside/deoxynucleotide pools were analyzed by high pressure liquid chromatography as described (McKee *et al*., 2004).

RESULTS

Cytotoxicity and Time to Subculture for MOLT-3 Cells Exposed Chronically to AZT

MOLT-3 cells that were collected 24 h after exposure to 0, 10, or 800μM AZT exhibited a survival of 100, 81.9, and 69.2%, respectively. In separate experiments, time to subculture was assessed in MOLT-3 cells during the course of 14 passages of continuous exposure to 0, 10, or 800μM AZT (Fig. 1, open circles). In unexposed cells, passaging took place daily, and in AZT-exposed cells at P_2–P_5, a delay in the cell cycle was observed. However, Figure 1 shows that by five passages of AZT exposure, the rate of doubling was altered so that confluence was observed by 2-day intervals for P_5–P_{14}. Similar profile was observed for long-term MOLT-3 cells exposed to 10μM AZT.

During 14 passages of chronic exposure to 800μM AZT, the activity of TK-1, measured by the capacity to phosphorylate thymidine, revealed an abrupt decrease as early as P_1, which lasted until P_{14} (Fig. 1). Insets in Figure 1 show Western blots of monomeric (24 kDa) TK-1 from extracts obtained at the same passages for which time to confluence and activity were measured. The inserts show unexposed cells and cells exposed to AZT for the passages indicated and were obtained from the

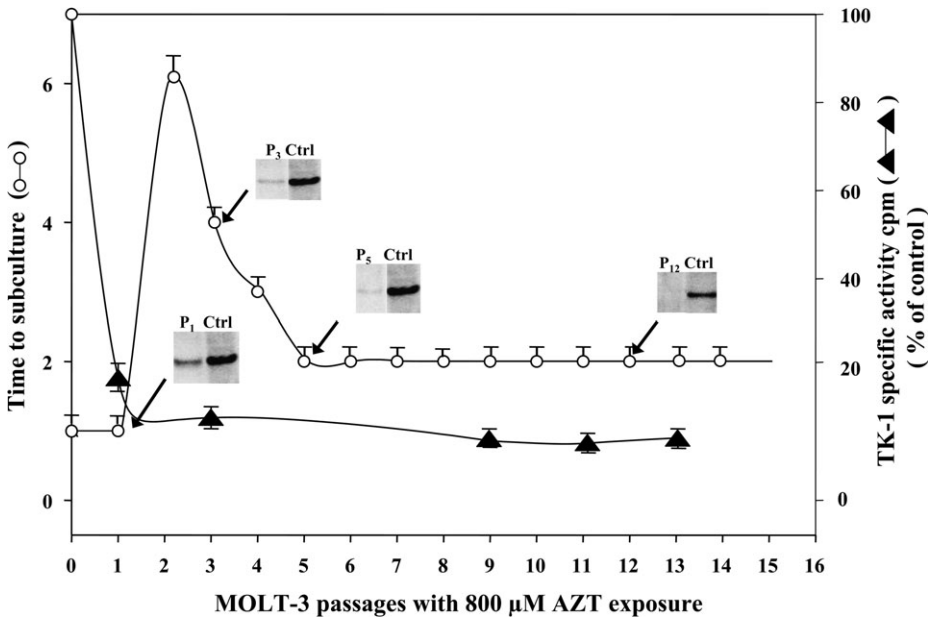

FIG. 1. Comparison of time to confluence (circles) and TK-1–specific activity (% of control [triangles]) for MOLT-3 cells exposed continuously to 800μM AZT. Time to confluence was determined visually, and TK-1 phosphorylation was obtained by radiolabeling assay (see ''Materials and Methods'' section). Insets show expression of monomeric 24-kDa TK-1 by Western blots, where the ''ctrl'' cells were unexposed and the exposed passages are indicated. For loading control, see Figure 5.

Western blot presented in Figure 5a. The reduction of TK-1 activity with continued culture time in the presence of AZT is clearly documented here.

Incorporation of AZT into MOLT-3 Cell DNA

An RIA was used to determine the amount of AZT incorporated into DNA at different passages. Figure 2 shows AZT-DNA incorporation values for MOLT-3 cells exposed to 5, 10, 50, 100, 200, and 800μM AZT for 1, 5, and 14 passages. Incorporation of AZT was observed at all passages with all doses, with maximum incorporation, 246 molecules AZT/10^6 nucleotides, at P_5 with the 200μM dose. For the 800μM AZT dose, the highest incorporation was also observed at P_5 with 171 molecules AZT/10^6 nucleotides. Figure 2 shows no obvious dose response either with dose or with increasing passage number. In an additional experiment, MOLT-3 cells originally exposed to 800μM AZT for 14 passages were subsequently cultured in AZT-free media, for an additional 12 passages. No detectable AZT-DNA incorporation remained after these cells were cultured in the absence of AZT for 12 passages (data not shown).

Statistical Interpretation

Application of linear regression to the mean levels of AZT-DNA incorporation at P_1 showed a positive trend with an R value of 0.737. However, the data did not pass the normality test ($p = 0.03$) due to the mean value at 10μM AZT. If the latter value for 10μM AZT is excluded, then the data for the remaining AZT concentrations pass a Normality Test, and a highly positive linear regression ($R = 0.985$) is observed at P_1. One-way ANOVA was used in addition to the Student's t-test to compare the data among groups on the MN experiments (Table 2), and the p value was of 0.0001.

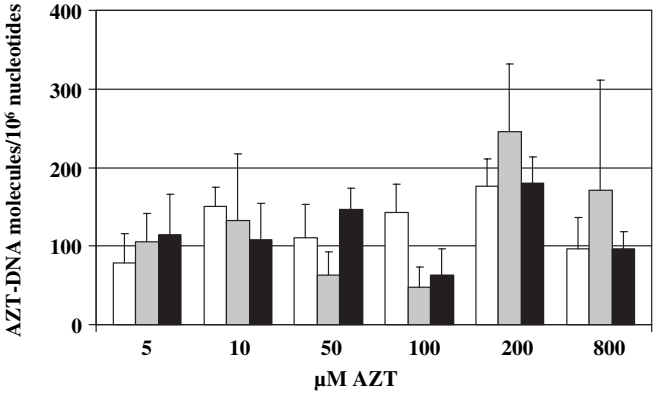

FIG. 2. AZT-DNA incorporation measured by an AZT-specific RIA. AZT-DNA incorporation for MOLT-3 cells exposed to 0, 5, 10, 20, 100, 200, and 800μM AZT at P_1 (white bars), P_5 (gray bars), and P_{14} (black bars). Each column shows the number of molecules of AZT incorporated into MOLT-3 cell DNA from cells exposed continuously to each dose. Values are mean ± SD from three experiments.

DNA Damage Assessed by the MN Assay

The MN assay was performed as one indicator of AZT-induced DNA damage. The induction of MN in MOLT-3 cells exposed to 10μM AZT (Fig. 3) and 800μM AZT (Fig. 3) is shown for passages 0, 1, 4, 5, and 14. In Figure 3 statistically significant differences were observed for all the AZT-exposed passages compared to the unexposed controls (p values = 0.016, 0.0003, 0.0078, and 0.0022 for P_1, P_4, P_5, and P_{14}, respectively). Additionally, a comparison among the unexposed controls cultured in parallel for P_1, P_4, P_5, and P_{14} showed no statistical significance ($p = 0.084$)

In cells exposed to 800μM AZT at P_1, P_4, P_5, and P_{14}, the MN (per 1000 cells examined) reached values of 20, 61, 38, and 35, respectively, a significant increase for passage 1 ($p = 0.02$) compared to the untreated control (P_U) and highly significant increase for P_4 ($p = 0.0001$), P_5 ($p = 0.0002$), and P_{14} ($p = 0.0001$); $p < 0.05$ for each passage compared to P_U. However at P_{27}, after 13 passages of culturing in the absence of drug, MN values returned to control levels (8/1000 cells) (Table 2).

Cell Cycle Analysis of MOLT-3 Cells Exposed Chronically to 800μM AZT

Evaluation of changes in the MOLT-3 cell cycle profile was carried out by flow cytometry in cells exposed long term to AZT. Table 1 shows percentages of cells in G_0–G_1, S, and G_2 phases determined in untreated (control) cells and in cells exposed to 800μM AZT at P_1 and P_{14}. Table 1 also shows values for cells at P_{24}, which were exposed to AZT for 15

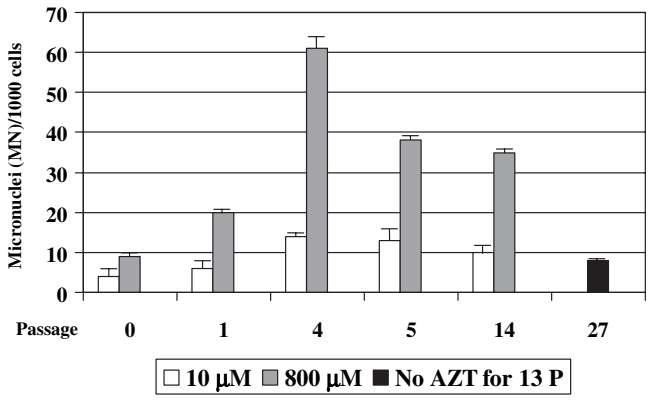

FIG. 3. Frequency of MN (MN cells/1000 MOLT-3 cells). MN were scored at P_0, P_1, P_4, P_5, and P_{14} of exposure to 10μM AZT (white bars), 800μM AZT (gray bars), and in cells at P_{27} (14 passages with 800μM AZT and 13 consecutive passages with no AZT, dark bar). Values are mean ± SD from three experiments. Comparison of MN induced by 10μM AZT frequency by Student's t-test showed a significant increase for passage 1 ($p = 0.016$) compared to the untreated control (P_0), P_4 ($p = 0.0003$), P_5 ($p = 0.0078$), and P_{14} ($p = 0.0022$). Values are mean ± SD from three experiments. Comparison of MN frequency induced by 800μM AZT by Student's t-test showed a significant increase for passage 1 ($p = 0.02$) compared to the untreated control (P_0) and highly significant increase for P_4 ($p = 0.0001$), P_5 ($p = 0.0002$), and P_{14} ($p = 0.0001$).

TABLE 1
Cell Cycle Analysis (flow cytometry) for MOLT-3 Cells Exposed to 800μM AZT for 14 Passages and No Drug for an Additional 10 Passages

	Control (P_0)	P_1	P_{14}	P_{24}
% Cells in G_1	46.5 ± 0.9	30.0 ± 2.6*	41.8 ± 3.4*	42.9 ± 1.0*
% Cells in S	42.7 ± 1.9	57.3 ± 3.0*	46.0 ± 2.5*	46.2 ± 0.9*
% Cells in G_2	11.4 ± 1.6	12.7 ± 0.5	12.1 ± 1.0	11.1 ± 0.2

Note. *p Values < 0.05 (Student's t-test). Values are mean ± SD for three experiments where AZT-exposed cells at P_1, P_{14}, and P_{24} were compared to the unexposed control.

passages and grown for 10 subsequent passages in medium without AZT. An accumulation of cells in S-phase was observed with AZT exposure and was not reversed during growth for 10 passages in the absence of AZT. The increase of cells in S-phase was accompanied by a decrease of cells in G_1. Although the most dramatic AZT-induced S-phase change was from 42 to 57% observed at P_1, cells at P_{14} and P_{24} also exhibited a statistically significant increase in S-phase accumulation. A marked decrease in percent of cells in G_1 was found for cells exposed to 800μM AZT for a single passage; 30% of AZT-exposed cells at P_1 were in G_1 compared to 46% of unexposed cells at P_0 in G_1 ($p = 0.05$) (Tables 1 and 2). Additionally, P_1 cells in G_1 and S-phase were altered more substantially than cells at P_{14} and P_{26}.

Reduction of TK-1 Protein Level with Long-term Culture of MOLT-3 Cells in the Presence of AZT

Cell lysates from consecutive passages of MOLT-3 cells exposed to 800μM AZT were processed for Western blot analysis using an anti-TK-1 antibody. Figure 4 shows the expression of TK-1 protein in its inactive dimeric (48 kDa) and active monomeric (24 kDa) forms, for unexposed (P_0) cells and cells exposed to 800μM AZT from P_1 to P_{14} as well as cells grown subsequently in AZT-free media (P_{17}–P_{19}). The 24-kDa band indicates the presence of active protein in cultures that have been either unexposed (control) or exposed to AZT for 24 h. Reduction in protein band intensity is apparent during subsequent passages 9–14 with AZT in the medium and passages 17–19 with no AZT. The inactive dimeric form, however, remains unchanged through P_{14} (Fig. 4). Cells at P_{15}–P_{19}, which were grown in AZT-free media after 14 passages of AZT exposure, exhibited a persistent loss of the TK-1 monomeric and dimeric forms and gain of a tetrameric 96-kDa form (Fig. 4). Figure 5b shows monomeric forms of TK-1 at P_1 and P_6 exposed to 5, 10, and 50μM AZT. P_U represents parallel untreated cultures sacrificed at either P_1 or P_6. The reduction of the 24-kDa form is visible at P_6 but not at P_1 with the low doses used in this experiment (representative of three experiments). Protein load is revealed by the actin loading control.

TK-1 Enzyme–Specific Activity

The oligomerization of TK-1, from monomer to dimer and tetramer, prompted us to investigate TK-1 phosphorylation–specific activity, and the data are shown in Figure 1 (solid triangles). An 80% decrease in TK-1 activity was observed in MOLT-3 cells at P_1 in the presence of 800μM AZT. During 13 consecutive passages, in which cells were cultured in the presence of 800μM AZT, TK-1 activity remained near the assay limit of detection (Fig. 1, Table 2). A plot of the relationship between the phosphorylation activity of TK-1 and time to confluence is shown in Figure 1, with insets indicating TK-1 protein levels determined by Western blot at P_1, P_3, P_5, and P_{12}. The Western blot insets also show that the drop in

TABLE 2
Comparison of Cell Cycle, Doubling Time, MN, and AZT-DNA Incorporation in P_0, P_1, P_5, and P_{14} MOLT-3 Cells Exposed to 800μM AZT

						MN/1000[b] cells	
Passage	Time to confluence (days)	S-phase (% cells)*	TK-1 activity (%)	TK-1 24-kDa	AZT/DNA[a]	10μM AZT[b,**]	800μM AZT***
P_0	1	43	100	+++	0	4	9
P_1	6	57	18	++	95	6	20
P_5	2	50	0	+	175	13	38
P_{14}	2	46	0	−	95	10	35
$P_{24–27}$	2	46	NA	−	0	—	8

Note. NA, not assayed.
[a]Measured in molecules AZT/10^6 nucleotides.
[b]ANOVA: $p = 0.0001$ control (P_U: average of untreated controls for P_1, P_4, P_5, and P_{14}) versus 10μM AZT P_1, P_4, P_5, and P_{14}.
*$p < 0.05$ for P_1, P_{14}, and P_{24} compared to P_0 (Student's t-test).
**$p < 0.016$ for P_1, 0.008 for P_5, and 0.002 for P_{14} compared to P_0 (Student's t-test).
***$p < 0.02$ for P_1, 0.0002 for P_5, and 0.0001 for P_{14} compared to P_0 (Student's t-test).

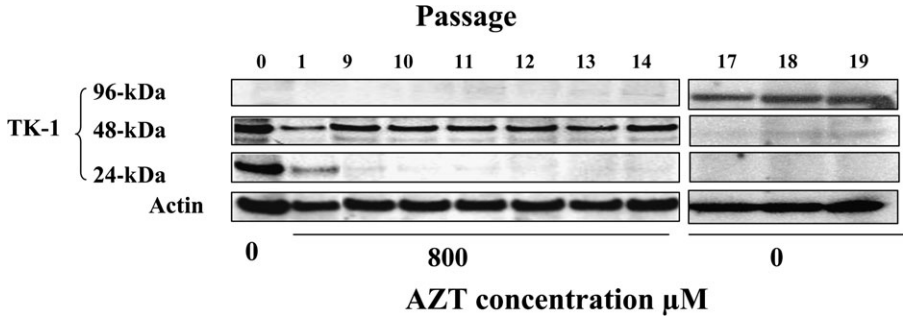

FIG. 4. TK-1 Western blot of MOLT-3 cells exposed to 0 (P_0) or to 800μM AZT (P_1–P_{14}) and cells grown subsequently (P_{17}–P_{19}) in the absence of AZT. The figure shows location of the active 24-kDa TK-1 and the inactive 48-kDa and 96-kDa forms of the enzyme as well as the actin loading control. This is a representative blot of three similar repeat experiments.

doubling time was accompanied by a loss of TK-1 monomeric protein (Fig. 1, P_1–P_5, and Fig. 5a).

Phosphorylation of Thymidine during Cell Growth

The data above suggested that in the presence of 800μM AZT, thymidine tri-phosphate (TTP) for DNA replication was provided predominantly from the *de novo* rather than the salvage pathway. To further assess this point, control cells and cells continually exposed to 800μM AZT at various passages were incubated with [^{3}H]-thymidine for 30 min, and the conversion to [^{3}H]-thymidine mono-phosphate, thymidine di-phosphate, and TTP was determined as described in "Materials and Methods" section. In the control cells, 60% of the label was phosphorylated, mostly to TTP (47%). After one passage in the presence of AZT, only a small amount of TTP (< 4% of total) was detected. At later passages, there was no detectable conversion of [^{3}H]-thymidine to [^{3}H]-TTP (data not shown).

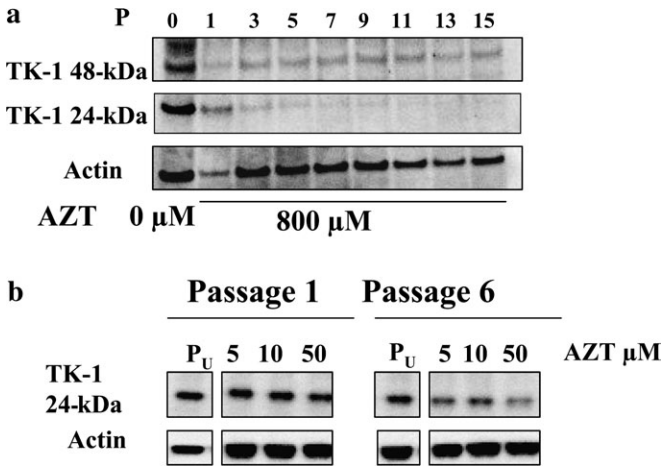

FIG. 5. (a) TK-1 Western blot of MOLT-3 cells exposed to 0 (P_0) or to 800μM AZT for 1, 3, 5, 7, 9, 13, and 15 passages. The figure shows location of the active 24-kDa TK-1 and the inactive 48-kDa form of the enzyme as well as the actin loading control. Bands of this blot have been used in Figure 1. (b) TK-1 Western blot of MOLT-3 cells exposed to 0 (P_U) or to 5, 10, and 50μM AZT for 1 and 6 passages. The figure shows location of the active 24-kDa TK-1 as well as the actin loading control.

Table 2 provides a summary of all the data presented in this paper. The doubling changes were similar to the percentage of cells in S-phase in that the cell cycle slowed immediately upon encountering the drug and subsequently ($\geq P_5$) shifted more toward normal. The TK-1–specific activity, in parallel with the TK-1 monomeric form, was completely depleted beyond P_5. However, the AZT-DNA incorporation and MN values were still high at P_{14} in the absence of active TK-1 and were only decreased after AZT was removed from the media.

DISCUSSION

The antiretroviral nucleoside analog AZT becomes incorporated intracellularly into the nascent HIV-1 viral DNA via reverse transcriptase and into the host DNA via classical polymerases (Furman *et al.*, 1986). Prior to this incorporation, the drug must be phosphorylated by TK-1, thymidylate kinase, and nucleoside diphosphate kinase (Furman *et al.*, 1986). In this report, an inhibition of TK-1 protein expression and activity was found to correlate with length of long-term AZT exposure in human lymphoblastoid MOLT-3 cells (Table 2). Incorporation of AZT into DNA, and more general DNA damage revealed by MN, were observed during AZT exposure and decreased to background levels when AZT was removed from the medium. The lack of dose response seen with AZT incorporation into the DNA MOLT-3 cells could be explained by the fact that these cells are derived from a patient who had received prior multidrug chemotherapy and has unusually high terminal deoxynucleotidyl transferase activity.

Cells cultured for 14 passages with 800μM AZT exhibited inhibition of TK-1 protein and phosphorylation activity along with cell cycle delay. Finally, when AZT was removed from the medium, active TK-1 did not recover and the cell cycle parameters did not return to normal, even though indicators of DNA damage, AZT incorporation, and MN returned to background levels. The dose used for most of the experiments presented here, 800μM AZT, is the highest dose with low cytotoxicity observed in this cell line. This high dose was employed in order to reveal mechanisms of AZT-induced

genotoxicity. In addition, using 10μM AZT, a dose found in human plasma of HIV-1–infected patients, we also found significant DNA damage (Fig. 3).

In agreement with the previous findings that only the monomeric form of TK-1 performs active phosphorylation (Sherley and Kelly, 1988), we observed a TK-1 phosphorylating activity on the part of the 24-kDa form of TK-1 (Fig. 1). The activity and the monomer disappeared after five passages of exposure to 800μM AZT and were not restored in further passages. In addition, the expression of the inactive dimeric form (48 kDa) remained unchanged as time of exposure to AZT increased (Fig. 1). Moreover, after AZT removal, the monomeric form was undetectable, the dimeric form was dramatically reduced, and a tetrameric form of 96 kDa became evident (Fig. 4, right panel). A modest reduction was observed when cells were exposed long term to lower doses as observed in Figure 5b.

Using a recombinant TK-1 model, others support the concept of a catalytically effective, ATP inducible tetrameric form with higher activity than the dimeric form (Munch-Petersen, 2009). Inhibition of TK-1 activity by AZT exposure has been reported in T-lymphocytic cells (Avramis *et al.*, 1993) and attributed to hypermethylation of the *TK-1* promoter (Wu *et al.*, 1995). Inhibition of the TK-1 enzyme has been reported to occur in HIV-1–infected patients (Antonelli *et al.*, 1996; Jacobsson *et al.*, 1995, 1998; Turriziani and Antonelli, 2004) as well. Antonelli *et al.* (1996) reported that 10 patients exposed to therapeutic doses of AZT for 6 months exhibited a significant reduction in the phosphorylation efficiency of the enzyme TK-1.

In H9 cells, the DNA methylation inhibitor 5-azacytidine reversed AZT-induced downregulation of *TK-1*, again suggesting that *TK-1* hypermethylation may account for the decreased *TK-1* gene expression (Groschel *et al.*, 2002; Hoever *et al.*, 2003). However, those reports do not discuss the form of the enzyme inhibited or the changes in oligomerization taking place after treatment.

Our data suggest that AZT induces the dimerization of the 24-kDa form (Fig. 4). Western blot analysis of long-term MOLT-3 cells exposed to 800μM AZT revealed the presence of a 24-kDa form and a 48-kDa form at earlier passages similar to the forms found in untreated cells. However, when exposure reached five passages, the 24-kDa form became undetectable and the 48-kDa form remained present. Furthermore, the only form present after removal of the drug for three to five passages was the 96-kDa tetramer (Fig. 4).

Interestingly, although TK-1 is considered to be the rate-limiting step in AZT incorporation into DNA, we measured incorporation at P_{14}, several passages after both the TK-1 activity and the monomer protein were undetectable. Three possible scenarios could explain this dichotomy. First, although undetectable by Western blots, low levels of TK-1 protein could have been sufficient to phosphorylate AZT that was been incorporated into DNA. Second, incorporation taken place at earlier passages, when an active form of TK-1 was present, could have remained in the DNA without being removed by DNA repair mechanisms and could have been present in later passages, perhaps in those cells with impaired or reduced cell division capacity. Finally, the nuclear encoded mitochondrial pyrimidine deoxynucleoside salvage enzyme TK-2, involved in pyrimidine nucleoside phosphorylation, could have been responsible for AZT phosphorylation in the absence of TK-1. Evidence of a phosphorylation activity for that enzyme has been reviewed by Eriksson *et al.* (2002), indicating that analogs, such as AZT, arabinofuranosylthymine, 3′-fluoro-2′,3′-deoxythymidine, and ribothymidine, could be phosphorylated but with relatively low efficiency. Evidence of this activity has been reported elsewhere utilizing transgenic mice that individually expressed pathogenetic point mutants of human TK-2 (Kohler *et al.*, 2008). TK-2 is constitutively expressed along the cell cycle and often is virtually the only thymidine kinase that is physiologically active in nonproliferating and resting cells (Perez-Perez *et al.*, 2008). To rule out nucleotide pool imbalances, experiments were performed employing equimolar concentrations of thymidine to study analysis of cell cycle and other end points. Results (Yu *et al.*, 2009) indicated that the doses of NRTIs used had no effect on the nucleotide pool.

It does not appear at the level of transcription, that salvage pathways have been activated, since the expression of the genes involved in this pathway, determined by microarray at P_1, P_5, and P_{14}, was unchanged in cells exposed after long term to AZT (data not shown).

Cell cycle abnormalities induced by AZT have been previously reported in human HeLa (Olivero *et al.*, 2005), HL60 (Roskrow and Wickramasinghe, 1990), and Jurkat cells (Wu *et al.*, 2004). Prior studies performed in our laboratory, using HeLa cells, revealed a delay in the cell cycle, with a dose-related significant increase in percentage of S-phase cell accumulation after 24 h of exposure to 63–500μM AZT. At 500μM AZT, there was a twofold increase in cells in S-phase. Here, we showed that AZT causes an accumulation of cells in S-phase accompanied by a decrease of cells in G_1 phase (Table 1). This difference was observed in cells exposed for 1 or 14 passages and was persistent for 10 passages after the drug was removed (P_{24}, Table 1). No difference was observed in the G_2-phase between the percentage of unexposed cells and AZT-exposed cells, for any of the passages analyzed.

In summary, this study showed that indicators of DNA damage, AZT-DNA incorporation, MN, and S-phase arrest occur in MOLT-3 cells exposed to AZT continuously for 15 passages, and only the S-phase arrest is not completely reversible in cells subsequently grown in AZT-free media. The study also showed that continuous AZT exposure resulted in an early (P_5) complete downregulation of the TK-1 24-kDa protein accompanied by a loss in the ability of TK-1 to phosphorylate AZT. The losses were not reversible at later passages after AZT was removed from the media. The data

showing AZT-induced DNA damage in the absence of active TK-1 were unexpected and requires explanation. The role of chronic AZT exposure as a modulator of TK-1 oligomerization and functional capacity could be relevant to AZT resistance in patients treated long term.

FUNDING

Intramural Research Program of the NIH, National Cancer Institute, Center for Cancer Research.

REFERENCES

Agarwal, R. P., and Olivero, O. A. (1997). Genotoxicity and mitochondrial damage in human lymphocytic cells chronically exposed to 3′-azido-2′,3′-dideoxythymidine (AZT). *Mutat. Res.* **390,** 223–231.

Antonelli, G., Turriziani, O., Verri, A., Narciso, P., Ferri, F., D'Offizi, G., and Dianzani, F. (1996). Long-term exposure to zidovudine affects in vitro and in vivo the efficiency of phosphorylation of thymidine kinase. *AIDS Res. Hum. Retroviruses* **12,** 223–228.

Arner, E. S., Spasokoukotskaja, T., and Eriksson, S. (1992). Selective assays for thymidine kinase 1 and 2 and deoxycytidine kinase and their activities in extracts from human cells and tissues. *Biochem. Biophys. Res. Commun.* **188,** 712–718.

Aruna, R., and Jagetia, G. C. (2001). Azidothymidine induces dose dependent increase in micronuclei formation in cultured HeLa cells. *Pharmazie* **56,** 492–500.

Avramis, V. I., Kwock, R., Solorzano, M. M., and Gomperts, E. (1993). Evidence of in vitro development of drug resistance to azidothymidine in T-lymphocytic leukemia cell lines (Jurkat E6-1/AZT-100) and in pediatric patients with HIV-1 infection. *J. Acquir. Immune Defic. Syndr.* **6,** 1287–1296.

Bishop, J. B., Witt, K. L., Tice, R. R., and Wolfe, G. W. (2004). Genetic damage detected in CD-1 mouse pups exposed perinatally to 3′-azido-3′-deoxythymidine and dideoxyinosine via maternal dosing, nursing, and direct gavage. *Environ. Mol. Mutagen.* **43,** 3–9.

Dertinger, S. D., Torous, D. K., and Tometsko, K. R. (1996). Induction of micronuclei by low doses of azidothymidine (AZT). *Mutat. Res.* **368,** 301–307.

Dobrovolsky, V. N., McGarrity, L. J., VonTungeln, L. S., Mittelstaedt, R. A., Morris, S. M., Beland, F. A., and Heflich, R. H. (2005). Micronucleated erythrocyte frequency in control and azidothymidine-treated Tk+/+, Tk+/- and Tk-/- mice. *Mutat. Res.* **570,** 227–235.

Eriksson, S., Munch-Petersen, B., Johansson, K., and Eklund, H. (2002). Structure and function of cellular deoxyribonucleoside kinases. *Cell. Mol. Life Sci.* **59,** 1327–1346.

Furman, P. A., Fyfe, J. A., St Clair, M. H., Weinhold, K., Rideout, J. L., Freeman, G. A., Lehrman, S. N., Bolognesi, D. P., Broder, S., Mitsuya, H., *et al.* (1986). Phosphorylation of 3′-azido-3′-deoxythymidine and selective interaction of the 5′-triphosphate with human immunodeficiency virus reverse transcriptase. *Proc. Natl. Acad. Sci. U.S.A.* **83,** 8333–8337.

Gonzalez, C. M., and Larripa, I. (1994). Genotoxicity of azidothymidine (AZT) in *in vitro* systems. *Mutat. Res.* **321,** 113–118.

Groschel, B., Kaufmann, A., Hover, G., Cinatl, J., Doerr, H. W., Noordhuis, P., Loves, W. J., Peters, G. J., and Cinatl, J., Jr. (2002). 3′-Azido-2′,3′-dideoxythymidine induced deficiency of thymidine kinases 1, 2 and deoxycytidine kinase in H9 T-lymphoid cells. *Biochem. Pharmacol.* **64,** 239–246.

Han, T., Fernandez, M., Sarkar, M., and Agarwal, R. P. (2004). 2′, 3′-Dideoxycytidine represses thymidine kinases 1 and 2 expression in T-lymphoid cells. *Life Sci.* **74,** 835–842.

Hoever, G., Groeschel, B., Chandra, P., Doerr, H. W., and Cinatl, J. (2003). The mechanism of 3′-azido-2′,3′-dideoxythymidine resistance to human lymphoid cells. *Int. J. Mol. Med.* **11,** 743–747.

The International Agency for Research on Cancer. (2000). *Some antiviral and antineoplastic drugs, and other pharmaceutical agents,* Vol. 76, pp. 73–127. World Health Organization. International Agency for Research on Cancer, Lyon, France. Monographs on the Evaluation of Carcinogenic Risks to Humans.

Jacobsson, B., Britton, S., He, Q., Karlsson, A., and Eriksson, S. (1995). Decreased thymidine kinase levels in peripheral blood cells from HIV-seropositive individuals: implications for zidovudine metabolism. *AIDS Res. Hum. Retroviruses* **11,** 805–811.

Jacobsson, B., Britton, S., Tornevik, Y., and Eriksson, S. (1998). Decrease in thymidylate kinase activity in peripheral blood mononuclear cells from HIV-infected individuals. *Biochem. Pharmacol.* **56,** 389–395.

Kohler, J. J., Hosseini, S. H., Green, E., Hoying-Brandt, A., Cucoranu, I., Haase, C. P., Russ, R., Srivastava, J., Ivey, K., Ludaway, T., *et al.* (2008). Cardiac-targeted transgenic mutant mitochondrial enzymes: mtDNA defects, antiretroviral toxicity and cardiomyopathy. *Cardiovasc. Toxicol.* **8,** 57–69.

McKee, E. E., Bentley, A. T., Hatch, M., Gingerich, J., and Susan-Resiga, D. (2004). Phosphorylation of thymidine and AZT in heart mitochondria: elucidation of a novel mechanism of AZT cardiotoxicity. *Cardiovasc. Toxicol.* **4,** 155–167.

Meng, Q., Su, T., O'Neill, J. P., and Walker, V. E. (2002). Molecular analysis of mutations at the HPRT and TK loci of human lymphoblastoid cells after combined treatments with 3′-azido-3′-deoxythymidine and 2′,3′-dideoxyinosinedagger. *Environ. Mol. Mutagen.* **39,** 282–295.

Mitsuya, H., Weinhold, K. J., Furman, P. A., St Clair, M. H., Lehrman, S. N., Gallo, R. C., Bolognesi, D., Barry, D. W., and Broder, S. (1985). 3′-Azido-3′-deoxythymidine (BW A509U): an antiviral agent that inhibits the infectivity and cytopathic effect of human T-lymphotropic virus type III/lymphadenopathy-associated virus in vitro. *Proc. Natl. Acad. Sci. U.S.A.* **82,** 7096–7100.

Mittelstaedt, R. A., Von Tungeln, L. S., Shaddock, J. G., Dobrovolsky, V. N., Beland, F. A., and Heflich, R. H. (2004). Analysis of mutations in the Tk gene of Tk(+/-) mice treated as neonates with 3′-azido-3′-deoxythymidine (AZT). *Mutat. Res.* **547,** 63–69.

Munch-Petersen, B. (2009). Reversible tetramerization of human TK1 to the high catalytic efficient form is induced by pyrophosphate, in addition to tripolyphosphates, or high enzyme concentration. *FEBS J.* **276,** 571–580.

Nyce, J., Leonard, S., Canupp, D., Schulz, S., and Wong, S. (1993). Epigenetic mechanisms of drug resistance: drug-induced DNA hypermethylation and drug resistance. *Proc. Natl. Acad. Sci. U.S.A.* **90,** 2960–2964.

Olivero, O. A. (2007). Mechanisms of genotoxicity of nucleoside reverse transcriptase inhibitors. *Environ. Mol. Mutagen.* **48,** 215–223.

Olivero, O. A., Beland, F. A., and Poirier, M. C. (1994). Immunofluorescent localization and quantitation of 3′-azido-2′, 3′-dideoxythymidine (AZT) incorporated into chromosomal DNA of human, hamster and mouse cell lines. *Int. J. Oncol.* **4,** 49–54.

Olivero, O. A., Ming, J. M., Das, S., Vazquez, I. L., Richardson, D. L., Weston, A., and Poirier, M. C. (2008). Human inter-individual variability in metabolism and genotoxic response to zidovudine. *Toxicol. Appl. Pharmacol.* **228,** 158–164.

Olivero, O. A., Tejera, A. M., Fernandez, J. J., Taylor, B. J., Das, S., Divi, R. L., and Poirier, M. C. (2005). Zidovudine induces S-phase arrest and cell cycle gene expression changes in human cells. *Mutagenesis* **20,** 139–146.

Perez-Perez, M. J., Priego, E. M., Hernandez, A. I., Familiar, O., Camarasa, M. J., Negri, A., Gago, F., and Balzarini, J. (2008). Structure, physiological role, and specific inhibitors of human thymidine kinase 2 (TK2): present and future. *Med. Res. Rev.* **28,** 797–820.

Richman, D. D., Fischl, M. A., Grieco, M. H., Gottlieb, M. S., Volberding, P. A., Laskin, O. L., Leedom, J. M., Groopman, J. E., Mildvan, D., and Hirsch, M. S. (1987). The toxicity of azidothymidine (AZT) in the treatment of patients with AIDS and AIDS-related complex. A double-blind, placebo-controlled trial. *N. Engl. J. Med.* **317,** 192–197.

Roskrow, M., and Wickramasinghe, S. N. (1990). Acute effects of 3′-azido-3′-deoxythymidine on the cell cycle of HL60 cells. *Clin. Lab. Haematol.* **12,** 177–184.

Sherley, J. L., and Kelly, T. J. (1988). Human cytosolic thymidine kinase. Purification and physical characterization of the enzyme from HeLa cells. *J. Biol. Chem.* **263,** 375–382.

Stern, M., Cid, M. G., Larripa, I., and Slavutsky, I. (1994). AZT-induction of micronuclei in human lymphocyte subpopulations. *Toxicol. Lett.* **70,** 235–242.

Turriziani, O., and Antonelli, G. (2004). Host factors and efficacy of antiretroviral treatment. *New Microbiol.* **27**(Suppl. 1), 63–69.

Von Tungeln, L. S., Dobrovolsky, V. N., Bishop, M. E., Shaddock, J. G., Heflich, R. H., and Beland, F. A. (2004). Frequency of Tk and Hprt lymphocyte mutants and bone marrow micronuclei in mice treated neonatally with zidovudine and didanosine. *Mutagenesis* **19,** 307–311.

Witt, K. L., Tice, R. R., Wolfe, G. W., and Bishop, J. B. (2004). Genetic damage detected in CD-1 mouse pups exposed perinatally to 3′-azido-3′-deoxythymidine or dideoxyinosine via maternal dosing, nursing, and direct gavage: II. Effects of the individual agents compared to combination treatment. *Environ. Mol. Mutagen.* **44,** 321–328.

Wu, S., Liu, X., Solorzano, M. M., Kwock, R., and Avramis, V. I. (1995). Development of zidovudine (AZT) resistance in Jurkat T cells is associated with decreased expression of the thymidine kinase (TK) gene and hypermethylation of the 5′ end of human TK gene. *J. Acquir. Immune Defic. Syndr. Hum. Retrovirol.* **8,** 1–9.

Wu, Y. W., Xiao, Q., Jiang, Y. Y., Fu, H., Ju, Y., and Zhao, Y. F. (2004). Synthesis, in vitro anticancer evaluation, and interference with cell cycle progression of N-phosphoamino acid esters of zidovudine and stavudine. *Nucleosides Nucleotides Nucleic Acids* **23,** 1797–1811.

Yarchoan, R., Mitsuya, H., Myers, C. E., and Broder, S. (1989). Clinical pharmacology of 3′-azido-2′,3′-dideoxythymidine (zidovudine) and related dideoxynucleosides. *N. Engl. J. Med.* **321,** 726–738.

Yu, M., Ward, Y., Poirier, M. C., and Olivero, O. A. (2009). Centrosome amplification induced by the antiretroviral nucleoside reverse transcriptase inhibitors lamivudine, stavudine, and didanosine. *Environ. Mol. Mutagen.* **50,** 718–724.